4.2. Classical Fear Conditioning

4.2.1 Contextual and Cued Test

Twenty mice (wild type, n = 10; *Arc*/*Arg*3.1 deficient, n = 10; 9 weeks of age) were used. This test consisted of three parts: a conditioning trial, a context test trial, and a cued test trial. Fear conditioning was carried out on a clear plastic chamber equipped with a stainless-steel grid floor (34 × 26 × 30 [H] cm). The luminance of the floor was 225 Lux in the conditioning and context test trial and 0–1 Lux in the cued test trial. A CCD camera was installed on the ceiling of the chamber and was connected to a video monitor and a Windows PC. The grid floor was wired to a shock generator. White noise (65 dB) was supplied from a loudspeaker as an auditory cue (conditioned stimulus, CS). The conditioning trial consisted of a 2-min exploration period followed by two CS–unconditioned stimulus (US) pairings separated by 1 min each. A US (foot-shock: 0.5 mA, 2 sec) was administered at the end of the 30-sec CS period. A context test was performed in the same conditioning chamber for 3 min in the absence of the white noise 24 hr after the conditioning trial. In addition, a cued test was performed in an alternative context with distinct cues: the test chamber was different from the conditioning chamber in brightness (dark environment, almost 0–1 Lux), color (white), floor structure (no grid), and shape (triangular). The cued test was conducted 24 hr after the contextual test was finished, and consisted of a 2-min exploration period (no CS) to evaluate the nonspecific contextual fear followed by a 2-min CS period (no foot shock) to evaluate the acquired cued fear.

4.2.2. STM and LTM test

A second set of mice (wild type, n = 10; *Arc*/*Arg*3.1 deficient, n = 10; 9 weeks of age) was used for these tests. The conditioning trial was the same as in the above contextual and cued test (see 4.2.1). After 4 hr, an STM test was conducted, and LTM tests were conducted 24 hr, 1 week, and 4 weeks later. STM and LTM tests were the same as the context test of 4.2.1. In this test, the cued test was not conducted to exclude any sensitization effect caused by the auditory cue.

4.2.3. Remote memory test

A third set of mice (wild type, n = 10; *Arc*/*Arg*3.1 deficient, n = 10; 9 weeks of age) was used. The conditioning trial was the same as in the above STM and LTM test (see 4.2.2). In this test, a context test was conducted 4 weeks after the conditioning trial.

Both the contextual and cued tests and the STM and LTM tests were replicated five times to confirm their reproducibility. The rate of the freezing response (immobility excluding respiration and heartbeat) of mice was measured as an index of fear memory. Data were collected and analyzed with Image J FZ2 (O'Hara, Tokyo, Japan; Image J XX is modified software based on the public domain Image J program developed at the U.S. National Institutes of Health and is available at http://rsb.info.nih.gov/ij).

4.3. Immunohistochemical Analysis

Brains (n = 4 male mice per group) were fixed with methacarn fixative (methanol/chloroform/acetic acid, 60:30:10 [v/v]), and paraffin-embedded sections were prepared [39]. Mouse monoclonal anti-neurofilament (NF-M, sc-20013; Santa Cruz Biotechnology, CA, USA; 1:1000; a marker for axons), rabbit polyclonal anti-microtubule-associated protein 1A (MAP1A, sc-25728; Santa Cruz Biotechnology; 1:1000; a marker for dendrites), mouse monoclonal anti-synaptophysin (SYP, sc-17750; Santa Cruz Biotechnology; 1:1000; a presynaptic marker), rabbit polyclonal anti-homer (HOM, sc-15321; Santa Cruz Biotechnology; 1:500; a postsynaptic marker), and anti-GluR1(GluR1, sc-28779; Santa Cruz Biotechnology; 1:500) were used for immunohistochemistry. Sections were pretreated with HistoVT-One (Nacalai Tesque, Japan) and incubated with primary antibodies. Signals were visualized with Alexa 568-conjugated anti-mouse IgG and Alexa 488-conjugated anti-rabbit IgG (Molecular Probes, OR). Images were obtained with an FV-300 confocal laser-scanning microscope (Olympus, Japan).

For semi-quantitative analysis of image, the ratio of fluorescence intensity was calculated and compared *Arc*/*Arg*3.1-deficient mice to wild-type by using IMAGE J program (http://rsb.info.nih.gov/ij/index.html. National Institute of Health, Bethesda), after adjusting background noise (n = 4 images per mouse).

5. ACKNOWLEDGEMENTS

We thank Dr. Yoshitake Sano for his comments and suggestions regarding this study. We also thank Dr. Mariko Katayama for her assistance in maintaining the *Arc*/*Arg*3.1-deficient mouse line.

REFERENCES

[1] Guzowski, J., Lyford, G., Stevenson, G., *et al.* (2000) Inhibition of activity-dependent Arc protein expression in the rat hippocampus impairs the maintenance of long-term potentiation and the consolidation of long-term memory. *The Journal of Neuroscience*, **20**, 3993-4001.

[2] Plath, N., Ohana, O., Dammermann, B., *et al.* (2006) *Arc*/*Arg*3.1 is essential for the consolidation of synaptic plasticity and memories. *Neuron*, **52**, 437-444.

[3] Chowdhury, S., Shepherd, J.D., Okuno, H., *et al.* (2006) *Arc*/*Arg*3.1 interacts with the endocytic machinery to regulate AMPA receptor trafficking. *Neuron*, **52**, 445-459.

[4] Rial Verde, E.M., Lee-Osbourne, J., Worley, P.F., *et al.*

(2006) Increased expression of the immediate-early gene arc/arg3.1 reduces AMPA receptor-mediated synaptic transmission. *Neuron*, **52**, 461-74.

[5] Shepherd, J.D., Rumbaugh, G., Wu, J., Chowdhury, S., *et al.* (2006) *Arc/Arg*3.1 mediates homeostatic synaptic scaling of AMPA receptors. *Neuron*, **52**, 475-84.

[6] Steward, O. and Worley, P. (2002) Local synthesis of proteins at synaptic sites on dendrites: role in synaptic plasticity and memory consolidation? *Neurobiology of Learning and Memory*, **78**, 508-527.

[7] Lyford, G., Yamagata, K., Kaufmann, W., *et al.* (1995) Arc, a growth factor and activity-regulated gene, encodes a novel cytoskeleton-associated protein that is enriched in neuronal dendrites. *Neuron*, **14**, 433-445.

[8] Rodríguez, J.J., Davies, H.A., Silva, A.T., *et al.* (2005) Long-term potentiation in the rat dentate gyrus is associated with enhanced *Arc/Arg*3.1 protein expression in spines, dendrites and glia. *European Journal of Neuroscience*, **21**, 2384-2396.

[9] Steward, O, and Worley, P. (2001) A cellular mechanism for targeting newly synthesized mRNAs to synaptic sites on dendrites. *Proceedings of the National Academy of Sciences of the United States of America*, **98**, 7062-7068.

[10] Fosnaugh, J., Bhat, R., Yamagata, K., *et al.* (1995) Activation of arc, a putative "effector" immediate early gene, by cocaine in rat brain. *Journal of Neurochemistry*, **64**, 2377-2380.

[11] Kodama, M., Akiyama, K., Ujike, H., *et al.* (1998) A robust increase in expression of arc gene, an effector immediate early gene, in the rat brain after acute and chronic methamphetamine administration. *Brain Research*, **796**, 273-283.

[12] Moro, H., Sato, H., Ida, I., *et al.* (2007) Effects of SKF-38393, a dopamine D1 receptor agonist on expression of amphetamine-induced behavioral sensitization and expression of immediate early gene arc in prefrontal cortex of rats. *Pharmacology Biochemistry and Behavior*, **87**, 56-64.

[13] Yamagata, K., Suzuki, K., Sugiura, H., *et al.* (2000) Activation of an effector immediate-early gene arc by methamphetamine. *Annals of the New York Academy of Sciences*, **914**, 22-32.

[14] Nakahara, T., Kuroki, T., Hashimoto, K., *et al.* (2000) Effect of atypical antipsychotics on phencyclidine-induced expression of arc in rat brain. *NeuroReport*, **11**, 551-555.

[15] Kremerskothen, J., Wendholt, D., Teber, I., *et al.* (2002) Insulin-inducedexpression of the activity-regulated cytoskeleton-associated gene (ARC) in human neuroblastoma cells requires p21(ras), mitogen-activated protein kinase/extracellular regulated kinase and src tyrosine kinases but is protein kinase C-independent. *Neuroscience Letters*, **22**, 153-156.

[16] Kunizuka, H., Kinouchi, H., Arai, S., *et al.* (1999) Activation of Arc gene, a dendritic immediate early gene, by middle cerebral artery occlusion in rat brain. *NeuroReport*, **10**, 1717-1722.

[17] Larsen, M.H., Olesen, M., Woldbye, D.P., *et al.* (2005) Regulation of activity-regulated cytoskeleton protein (Arc) mRNA after acute and chronic electroconvulsive stimulation in the rat. *Brain Research*, **1064**, 161-165.

[18] Mikkelsen, J. D. and Larsen, M. H. (2006) Effects of stress and adrenalectomy on activity-regulated cytoskeleton protein (Arc) gene expression. *Neuroscience Letters*, **403**, 239-243.

[19] Guthrie, K., Rayhanabad, J., Kuhl, D., *et al.* (2000) Odors regulate Arc expression in neuronal ensembles engaged in odor processing. *NeuroReport*, **11**, 1809-1813.

[20] [20] Matsuoka, M., Yamagata, K., Sugiura, H., *et al.* (2002) Expression and regulation of the immediate-early gene product Arc in the accessory olfactory bulb after mating in male rat. *Neuroscience*, **11**, 251-258.

[21] Montag-Sallaz, M, and Montag, D. (2003) Learning-induced arg 3.1/arc mRNA expression in the mouse brain. *Learning and Memory*, **10**, 99-107.

[22] Kelly, M.P. and Deadwyler, S.A. (2003) Experience-dependent regulation of the immediate-early gene arc differs across brain regions. *The Journal of Neuroscience*, **23**, 6443-6451.

[23] Taishi, P., Sanchez, C., Wang, Y., *et al.* (2001) Conditions that affect sleep alter the expression of molecules associated with synaptic plasticity. *American Journal of Physiology: Regulatory Integrative and Comparative Physiology*, **281**, R839-R845.

[24] Kelly, M.P. and Deadwyler, S.A. (2002) Acquisition of a novel behavior induces higher levels of Arc mRNA than does overtrained performance. *Neuroscience*, **110**, 617-626.

[25] Ons, S., Martí, O. and Armario, A. (2004) Stress-induced activation of the immediate early gene Arc (activity-regulated cytoskeleton-associated protein) is restricted to telencephalic areas in the rat brain: relationship to c-fos mRNA. *Journal of Neurochemistry*, **89**, 1111-1118.

[26] Cook, E.H., Jr., Lindgren, V., Leventhal, B.L., *et al.* (1997) Autism or atypical autism in maternally but not paternally derived proximal 15q duplication. *The American Journal of Human Genetics*, **60**, 928-934.

[27] Glessner, J.T., Wang, K., Cai, G., Korvatsuka, O., *et al.* (2009) Autism genome-wide copy number variation reveals ubiquitin and neuronal genes. *Nature*, **459**, 569-573.

[28] Suteliffe, J.S., Nurmi, E.L. and Lombroso, P.J. (2003) Genetics of childhood disorders: XLVII. Autism, part 6: duplication and inherited susceptibility of chromosome 15q11-q13 genes in autism. *Journal of the American Academy of Child and Adolescent Psychiatry*, **42**, 253-256.

[29] Kishino, T., Lalande, M. and Wagstaff, J. (1997) UBE3A/E6-AP mutations cause Angeleman syndrome. *Nature Genetics*, **15**, 70-73.

[30] Matsuura, T., Sutcliffe, J. S., Fang, P., *et al.* (1997) De novo truncating mutations in E6-AP ubiquitin-protein ligase gene (UBE3A) in Angelman syndrome. *Nature Genetics*, **15**, 74-77.

[31] Greer, P.L., Hanayama, R., Bloodgood, B.L., *et al.* (2010). The Angelman Syndrome protein Ube3A regulates synapse development by ubiquitinating arc. *Cell*, **140**, 704-716.

[32] Radulovic, J., Kammermeir, J. and Spiess, J. (1998) Generalization of fear responses in C57BL/6J mice subjected to one-trial foreground contextual fear conditioning. *Behavioral Brain Research*, **95**, 179-189.

[33] Suzuki, A., Josselyn, S.A., Frankland, P.W., *et al.* (2004) Memory Reconsolidation and Extinction Have Distinct Temporal and Biochemical Signatures. *The Journal of Neuroscience*, **24**, 4787-4795.

[34] LeDoux, J. (1993) Emotional memory: in search of systems and synapses. *Annals of the New York Academy of Sciences*, **702**, 149-157.

[35] von Hertzen, L.S.J. and Giese, K.P. (2005) Memory Reconsolidation Engages Only a Subset of Immediate-Early Genes Induced during Consolidation. *The Journal of Neuroscience*, **25**, 1935-1942.

[36] MacDonald, J.F., Jackson, M.F. and Beazely, M.A. (2006) Hippocampal long-term synaptic plasticity and signal amplification of NMDA receptors. *Critical Reviews in Neurobiology*, **18**, 71-84.

[37] Sekiguchi, M., Yamada, K., Jin, J., *et al.* (2001) The AMPA receptor allosteric potentiator, PEPA ameliorates post-ischemic memory impairment. *NeuroReport*, **12**, 2947-2950.

[38] Yamada, D., Zushida, K., Wada, K., *et al.* (2009) Pharmacological Discrimination of Extinction and Reconsolidation of Contextual Fear Memory by a Potentiator of AMPA Receptors. *Neuropsychopharmacology*, **34**, 2574-2584

[39] Tanemura, K., Igarashi, K., Matsugami, T-R., *et al.* (2009) Intraurine environment-genome interaction and children's development (2): eBrain structure impairment and behavioral disturbance induced in male mice offspring by a single intraperitoneal administration of domoic acid (DA) to their dams. *The Journal of Toxicological Sciences*, **34**, SP279-286.

Abbreviations

Arc/Arg3.1: activity-regulated cytoskeleton-associated protein; LTP: long-term potentiation; LTM: long-term memory; STM: short-term memory; NF-M; neurofilament-M MAP1A; Microtubule-associated protein 1A; SYP; synaptophysin; HOM; homer; DG: dentate gyrus

SCIENTIFIC REPORTS

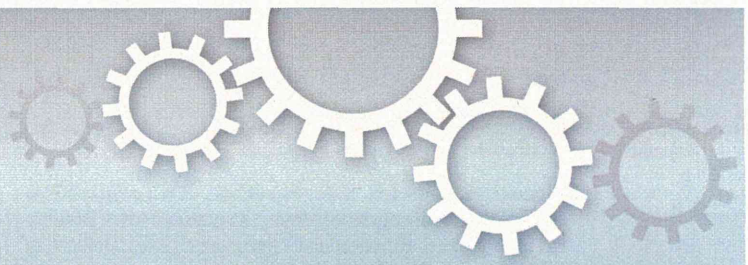

OPEN

SUBJECT AREAS:
BEHAVIOUR
GENETIC POLYMORPHISM
NEUROANATOMY
NEURODEVELOPMENTAL DISORDERS

Received
18 April 2011

Accepted
23 May 2011

Published
17 June 2011

Correspondence and requests for materials should be addressed to J.A. (jaruga@brain.riken.jp)

* These authors contributed equally to this work.

‡ Present address: Division of Molecular Biology, Institute of Medical Science, The University of Tokyo, Minato-ku, Tokyo 108-8639, Japan.

Zic2 hypomorphic mutant mice as a schizophrenia model and *ZIC2* mutations identified in schizophrenia patients

Minoru Hatayama[1]*, Akira Ishiguro[1]*‡, Yoshimi Iwayama[2], Noriko Takashima[1], Kazuto Sakoori[1], Tomoko Toyota[2], Yayoi Nozaki[1], Yuri S. Odaka[1], Kazuyuki Yamada[3], Takeo Yoshikawa[2] & Jun Aruga[1]

[1]Laboratory for Behavioral and Developmental Disorders, [2]Laboratory for Molecular Psychiatry, and [3]Support Unit for Animal Experiments, RIKEN Brain Science Institute, Wako-shi, Saitama 351-0198, Japan.

***ZIC2* is a causal gene for holoprosencephaly and encodes a zinc-finger-type transcriptional regulator. We characterized *Zic2*$^{kd/+}$ mice with a moderate (40%) reduction in *Zic2* expression. *Zic2*$^{kd/+}$ mice showed increased locomotor activity in novel environments, cognitive and sensorimotor gating dysfunctions, and social behavioral abnormalities. *Zic2*$^{kd/+}$ brain involved enlargement of the lateral ventricle, thinning of the cerebral cortex and corpus callosum, and decreased number of cholinergic neurons in the basal forebrain. Because these features are reminiscent of schizophrenia, we examined *ZIC2* variant-carrying allele frequencies in schizophrenia patients and in controls in the Japanese population. Among three novel missense mutations in ZIC2, R409P was only found in schizophrenia patients, and was located in a strongly conserved position of the zinc finger domain. Mouse Zic2 with the corresponding mutation showed lowered transcription-activating capacity and had impaired target DNA-binding and co-factor-binding capacities. These results warrant further study of ZIC2 in the pathogenesis of schizophrenia.**

Zic2/ZIC2 is a member of the Zic family of zinc finger proteins, which function as transcriptional regulators with critical roles in neural development[1–5]. In humans, haploinsufficiency of *ZIC2* results in holoprosencephaly (HPE)[6,7] in which the formation of medial forebrain structures is disturbed. *ZIC2* mutations are found in 3%–4% of unrelated individuals with isolated HPE[7]. Mice homozygous for a hypomorphic mutation in *Zic2* (*Zic2*$^{kd/kd}$) show embryonic or perinatal lethality with HPE-like symptoms and other anomalies[8–11], suggesting that the role of *Zic2* in forebrain development is largely conserved between human and mouse.

The role of Zic2 in embryonic development has been well-studied, but its role in the mature brain and/or the consequences of developmental Zic2 insufficiency in mature animals has not been fully investigated. It is possible that hypomorphic mutations that do not cause embryonic/perinatal lethality have a profound influence on higher brain functions. A pilot investigation analyzing the behavior of mice heterozygous for the hypomorphic mutation in *Zic2* (*Zic2*$^{kd/+}$) showed some abnormalities of the acoustic startle response[12]. However, the behaviors examined in that study were limited. A more comprehensive analysis is needed to clarify the causal relationship between the hypomorphic in *Zic2* and behavioral abnormalities that might underlie neuropsychiatric disorders such as schizophrenia.

Schizophrenia is a relatively common mental disorder that affects 1% of the population worldwide. The disease is characterized by positive symptoms (delusions and hallucinations), negative symptoms (affective flattening and social withdrawal), and cognitive dysfunction (deficits in working memory, attention, processing speed, and executive function)[13,14]. Morphologically, there are abnormalities of the brain that are frequently found in schizophrenia, such as enlarged ventricles, dendritic changes in the pyramidal neurons, and alteration of specific subtypes of interneurons[15–18]. Although the molecular basis of the disease is not fully understood, rare gene mutations that exert large effects in the susceptibility of schizophrenia, in addition to multiple common single nucleotide polymorphisms (SNPs), are being accumulated[19–22].

Here, we first performed comprehensive analyses of the *Zic2*$^{kd/+}$ mice in manifold behavioral test situations and by morphological and histological examinations. Then, since the results suggested that the *Zic2*$^{kd/+}$ mice mimic the schizophrenia-like phenotypes, we undertook resequencing analysis of the *ZIC2* gene using DNA isolated from patients with schizophrenia and from controls. One mutation, R409P, was shown to have impaired transcription activity, DNA-binding ability, and cofactor-binding capacity. These results were discussed in terms of the pathogenesis of schizophrenia.

Results

Wild-type ($Zic2^{+/+}$) and $Zic2^{kd/+}$ mice are indistinguishable by their body weight and external appearance[12]. Both male and female $Zic2^{kd/+}$ mice are fertile and female $Zic2^{kd/+}$ mice can foster their progenies without any obvious faults[8]. In our previous study, we found that prepulse inhibition (PPI) of acoustic startle response is decreased in $Zic2^{kd/+}$ mice[12]. For a more comprehensive analysis of behavioral phenotypes, we carried out the suite of behavioral tests listed in Table 1. For the light-dark box test, marble burying test, elevated plus maze test, forced swimming test, grip strength test, wire hanging test, footprint test and rotarod test, we found no significant differences in behavior between $Zic2^{kd/+}$ and wild-type mice (Table 1)[12]. For the remaining tests, we found significant differences in behavior between $Zic2^{kd/+}$ and wild-type mice; as described below.

Locomotor activities were lower or higher in $Zic2^{kd/+}$ mice than wild-type mice depending on the situation. We first placed the mice in new home cages and then monitored their locomotor activity continuously for 13 days (Figure 1A–C). Our analysis revealed that the locomotor activity was significantly lower in $Zic2^{kd/+}$ mice than in wild-type mice in the later stationary period (relatively low day-to-day variance, days 6–13) ($P = 0.044$) (Figure 1A). When we assessed the mean circadian locomotor activities during the stationary period, we found that the activity of $Zic2^{kd/+}$ mice was significantly lower than that of the wild type in the early dark phase (20:00–24:00) ($P = 0.048$), but that the circadian rhythm of the $Zic2^{kd/+}$ mice was normal (Figure 1B).

We also assessed locomotor activity in open field tests with observation times of 15 min. $Zic2^{kd/+}$ mice showed a significantly higher overall locomotor activity compared to wild-type mice ($P = 0.041$) (Figure 1C, left), but there were no differences in preference between the two genotypes for the central and peripheral fields (Figure 1C, right). These results suggest that $Zic2^{kd/+}$ mice have higher locomotor activities than the wild type in a novel environment.

Cognitive function deficits in $Zic2^{kd/+}$ mice. The Morris water maze test is commonly used to evaluate learning ability and acquisition of spatial memory. In our study, this test consisted of 4 days of training (day 1–4) with a fixed hidden platform, 1 day (day 5) of a probe test without a platform, and 1 day (day 6) of a reverse test in which the hidden platform was placed in the opposite quadrant. To reach the hidden platform, $Zic2^{kd/+}$ mice needed a significantly longer time in the training session ($P = 0.046$) and a significantly longer time in the reverse test session ($P = 0.037$) (Figure 2A, top panel). The moving speed of $Zic2^{kd/+}$ mice was slightly, and significantly, lower than that of wild-type mice only on day 1 of the training session (Figure 2A, left middle panel, $P = 0.036$). However, their spatial memory acquisition was not impaired as seen in the results of the probe test (Figure 2A, bottom panel). The motor performance and motivation of $Zic2^{kd/+}$ mice might not be impaired, given that there were no significant differences between the two genotypes in the moving speed at days 2 to 4 [$F(1,18) = 0.017$, $P = 0.90$, RMANOVA, main effect of genotype] (Figure 2A, left middle panel) or in the overall no movement time [$F(1,18) = 0.23$, $P = 0.64$, RMANOVA, main effect of genotype] (Figure 2A, right middle panel). Further supporting this notion, the results were similar for $Zic2^{kd/+}$ and wild-type mice for the other tests related to motor performance and motivation (rotarod, footprint, wire hanging and forced swimming test) (Table 1). Therefore, the water maze test results were considered to reflect an impaired learning ability of $Zic2^{kd/+}$ mice.

Fear conditioning is a test for associative learning that depends partly on hippocampal function, as is the Morris water maze test. The association of conditioned stimuli (CS, tone) and unconditioned noxious stimuli (US, electric foot shock) was learned in the conditioning on day 1. The results were quantitatively evaluated by the freezing response of the subjects. $Zic2^{kd/+}$ mice showed a significantly reduced freezing response in the context test on day 2 ($P = 0.037$, U-test, Figure 2B). These mice also showed a significantly reduced freezing response in the cue test on day 3 ($P = 0.049$, U-test, Figure 2C).

We also observed abnormal behavioral traits in $Zic2^{kd/+}$ mice in the Y-maze spontaneous alternation test. $Zic2^{kd/+}$ mice showed a significantly lower alteration percentage ($P = 0.046$, U-test) and a significantly higher number of arm entries ($P = 0.0040$) than the wild-type mice (Figure 2C), suggesting that $Zic2^{kd/+}$ mice have working memory impairment and a higher level of locomotor activity in a novel environment. Together with the absence of behavioral traits related to mood disturbances or anxiety-like behaviors, our results from the water maze, fear-conditioning and Y-maze tests are consistent with the impaired cognitive function in $Zic2^{kd/+}$ mice.

Abnormalities in social behavior in $Zic2^{kd/+}$ mice. We next assessed the social behaviors of the $Zic2^{kd/+}$ mice by the resident-intruder assay. Juvenile wild-type mice were placed into the home cages of

Table 1 | Summary of $Zic2^{kd/+}$ behavioral analysis.

Test	Response[1]	Implication to schizophrenia[2]
Home cage activity	decreased*	Negative?
Open field		
Locomotor	increased*	Positive (psychomotor agitation)
% center	no change	
Morris Water Maze		
Latency-training	increased*	
Latency-reverse	increased*	Cognitive (learning deficits)
Probe test	no change	
Speed-training	initially slow*	
No move-training	no change	
Fear conditioning		
Conditioning	no change	
Contextual	decreased*	Cognitive (fear memory deficits)
Cue	slightly decreased*	
Y-maze		
No. of entries	increased*	Positive (psychomotor agitation)
% alteration	decreased*	Cognitive (working memory deficits)
Social interaction		
Novel environment	no change	
Resident intruder	attack decreased*	Negative (social withdrawal)
Social dominance	often loser*	Negative (social withdrawal)
Social recognition	no change	
Acoustic startle response	increased*[3]	Cognitive (sensorimotor gating)
PPI of acoustic startle response	decreased*[3]	Cognitive (sensorimotor gating)
Light-Dark box	no change	
Marble burying	no change	
Burrowing	no change	
Elevated Plus maze	no change[3]	
Forced swimming	no change[3]	
Tail suspension	no change	
Grip strength	no change[3]	
Wire hanging	no change[3]	
Footprint	no change[3]	
Rotarod	no change[3]	

[1] $Zic2^{kd/+}$ compared to $Zic2^{+/+}$; [2] Possible relevance to the three classes of schizophrenia symptoms (positive, negative, and cognitive dysfunction); [3] Ogura et al. (2001) [12]; *$P < 0.05$ in statistical tests between $Zic2^{+/+}$ and $Zic2^{kd/-}$.

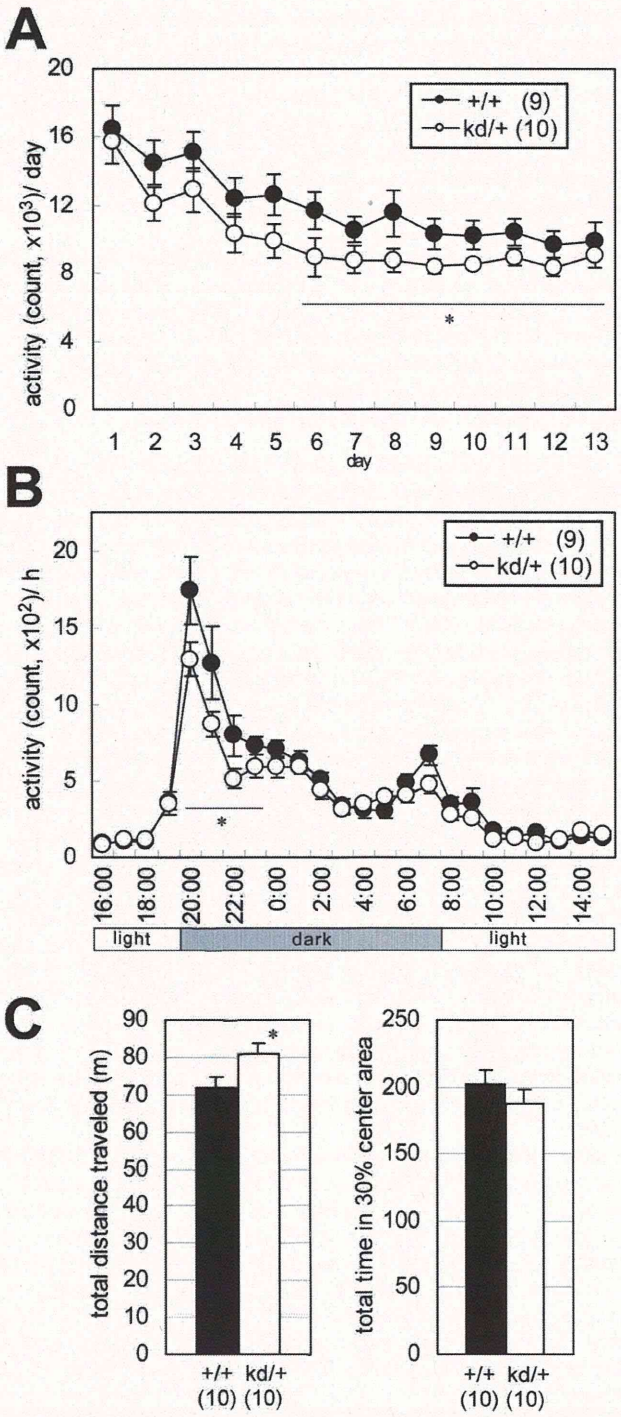

Figure 1 | Spontaneous motor performance abnormalities in *Zic2*$^{kd/+}$ mice. (A) Home cage activity was measured for 13 days. On day 1 the mice were put into a new home cage. Mean activities per day are indicated. Activity counts represent the number of time bins (approximately 0.20–0.25 s each) in which spontaneous activity including locomotor activity, rearing, and other activities such as stereotypic movements, were detected. *$P < 0.05$ in t-test. (B) Circadian activities. The values indicate the summation of the activities corresponding time bins (bin= 1 h) of the last 8 days (days 6–13) when the daily change in the total activity level (A) was minimal. *$P < 0.05$ in t-test. (C) Open field test. (left) Total distance traveled in the open box for 15 min observation period. (right) Percentage of the total time in the central area of the field (30% of the total field area). *$P < 0.05$ in t-test. Data is presented as means ± SEM. The number of mice in each group is given in parentheses.

the resident *Zic2*$^{kd/+}$ mice and the behavior of the test mice (*Zic2*$^{kd/+}$ mice or control wild-type mice) were analyzed for 15 min (Figure 3A, 3B, supplemental video). The time spent attacking ($P = 0.049$; Figure 3A, left panel) and the frequency of attacks were significantly lower in *Zic2*$^{kd/+}$ mice than in control wild-type mice ($P = 0.049$; Figure 3A, right panel). The frequency of body contact also tended to be higher in *Zic2*$^{kd/+}$ mice than in wild-type mice ($P = 0.12$). We also observed abnormal social behavior in *Zic2*$^{kd/+}$ mice in the social dominance tube test (Figure 3C). In this test, *Zic2*$^{kd/+}$ mice and control wild-type mice were placed at opposite ends of a transparent plastic tube in a head-to-head direction, and the first mouse to escape was judged the loser (Figure 3B). In general, mice of both genotypes moved forward and pushed each other within the tube. *Zic2*$^{kd/+}$ mice became losers more frequently than the wild-type mice ($P = 0.024$, chi-square test). We also performed a social interaction test in a novel environment (open field) with caged (Figure S1B) and non-caged partners (Figure S1A), but found no clear differences in the number and duration of the contacts between *Zic2*$^{kd/+}$ and wild-type mice.

Zic2$^{kd/+}$ mouse brain shows an altered morphology and reduction of forebrain cholinergic neurons and amygdalar Zic-positive cells. To elucidate the molecular basis of the behavioral abnormalities observed in *Zic2*$^{kd/+}$ mice, we performed a morphometric analysis of the *Zic2*$^{kd/+}$ mouse brain by MRI (Figure 4). We showed that *Zic2*$^{kd/+}$ mouse brains had enlarged lateral ventricles compared with the brains of wild-type mice (Figure 4A and B). The ratio of the volume of lateral ventricles to brain was 35% higher in the brains of *Zic2*$^{kd/+}$ mice than in those of wild-type mice. The 3D superimposition of lateral ventricles in the brain indicated that the enlargement was most notable in the anterior horn region (Figure 4B and C). Enlargement of the lateral ventricles in *Zic2*$^{kd/+}$ mice might partly reflect the reduction in the mass of the septum (Figure 4A, right panel), which we also observed in MRI 2D coronal images through the anterior commissure (data not shown). The hippocampal size did not show any clear differences between the two genotypes. Morphometric analysis of histological sections revealed that compared to the wild type the thickness of the cerebral cortex and the corpus callosum was slightly but significantly thinner in *Zic2*$^{kd/+}$ mice (cerebral cortex, $P = 0.0038$; corpus callosum, $P = 0.0028$; Figure 4D) and that the position and shape of the medial structure rostral to the hippocampus (fimbria including septofimbrial nucleus or septal triangular nucleus) were significantly narrower ($P < 0.001$ for both, Figure 4D).

We also found the amygdala in *Zic2*$^{kd/+}$ mice to be morphologically different to that in wild-type mice. In wild-type mice, Zic-positive cells were abundant in the amygdalohippocampal area (AHA) and sparse in the medial and cortical nuclei (Figure 4E). In *Zic2*$^{kd/+}$mice, the Zic-positive cells were less abundant than in wild-type mice in the equivalent rostrocaudal positions (Figure 4E, 8/8). Furthermore, the high cell density in the AHA of wild type animals shown in toluidine blue staining seemed reduced and the intense signals detected by acetylcholine esterase staining in the AHA was debilitated (Figure 4E), in *Zic2*$^{kd/+}$ mice. As shown by acetylcholine esterase stained sections (Figure 4E), in some cases (6/8), the medial protrusion of the amygdala in the coronal sections tended to be blunted in *Zic2*$^{kd/+}$ mice compared to the wild type.

The reduction of the septal mass and expression of *Zic2* in the basal forebrain structures[10] led us to investigate the number of cholinergic neurons that are densely distributed in the septum. We counted the choline acetyl transferase (ChAT)-positive cholinergic neurons in comparable coronal sections from the brains of *Zic2*$^{kd/+}$ and wild-type mice. The results indicated that the numbers of cholinergic neurons were decreased in the medial septum, diagonal band and substantia innominata regions, but not in other regions including cerebral cortex, striatum and caudoputamen, (Figure 5A–C). In

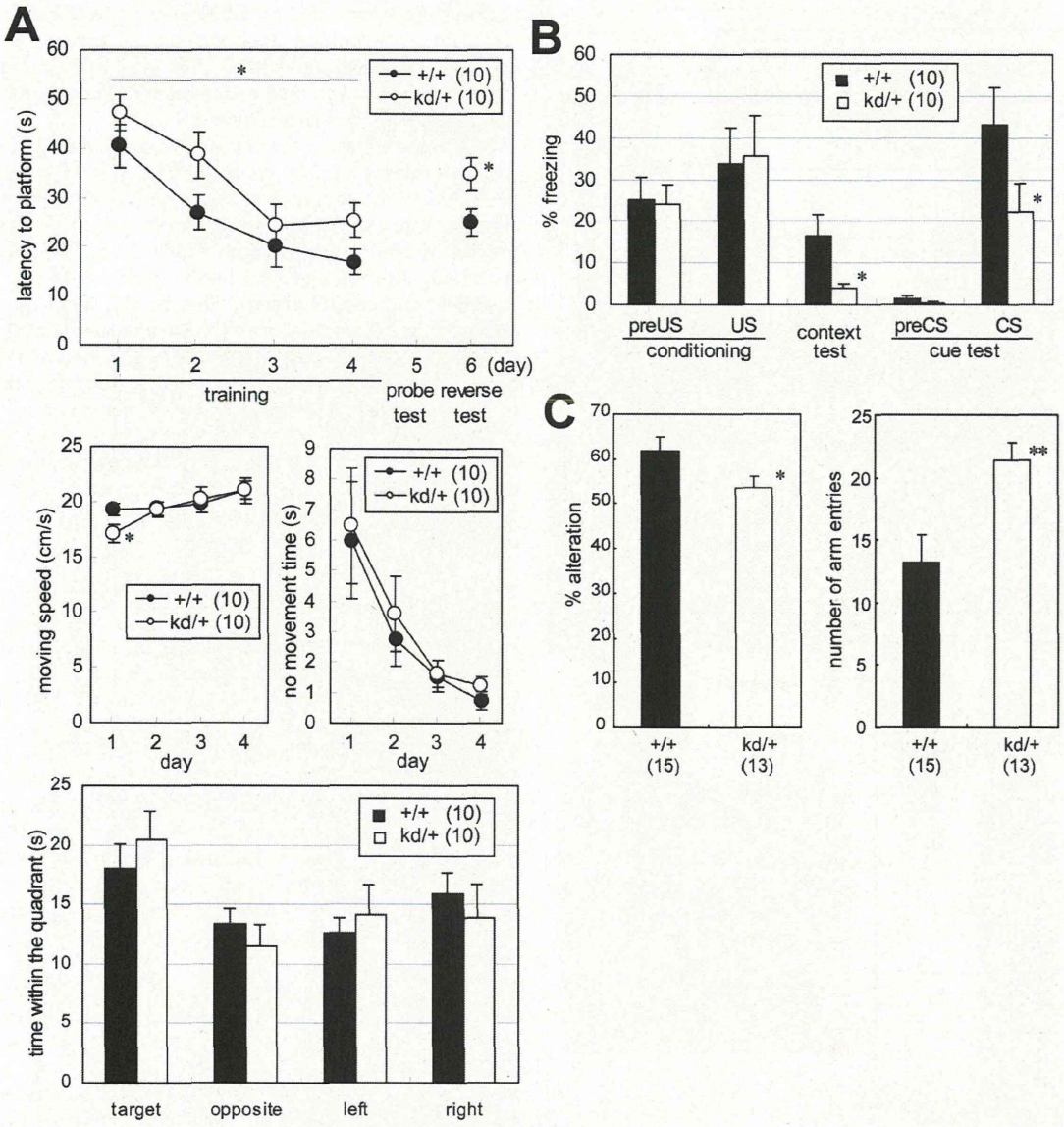

Figure 2 | Cognitive function deficits in *Zic2*$^{kd/+}$ mice. (A) Morris water maze test. (top) Mean latency to reach the platform during the training session (days 1–4) and reverse test session (day 6). Values indicate the mean of all six trials on the day. (middle left) Moving speed in the training session. (middle right) No movement time in the training session. (bottom) The results of the probe test (day 5) as indicated by the period of time (s) in the indicated quadrant within the 60 s testing period. *$P < 0.05$ in t-test. (B) Fear conditioning test. Mean percentage freezing are indicated for the conditioning test (day 1) before and after the electrical foot shock (preUS [mean of the 2 min before unconditioned-stimulus, US] and US [1 min after US] respectively), context test (day 2, mean of the total testing period [5 min]), and cue test (day 3) before and after pre tone (preCS [mean of the 2 min before conditioned stimulus, CS] and CS [mean of the 2 min with CS], respectively). *$P < 0.05$ in Mann-Whitney U-test. (C) Y-maze test. (left) Percentage altered selection of the entered arm. (right) Total number of arm entries. *$P < 0.05$ in Mann-Whitney U-test; **$P < 0.01$ in t-test. Data is presented as means ± SEM. The number of mice in each group is given in parentheses.

addition, the numbers of PV-positive neurons were not different in the medial septum or diagnonal band (Figure 5D). Therefore, the number of basal forebrain cholinergic neurons is selectively reduced by the reduction of *Zic2* expression. We also examined the number of ChAT-positive cells with or without Zic-like immunoreactivities in the affected regions (medial septum, diagonal band and substantia innominata) at early postnatal stages (P5–7, Figure 5E). In *Zic2*$^{kd/+}$ mice, we observed a significant reduction in the number of Zic$^-$ChAT$^+$ cells in the diagonal band region compared to the number in wild-type mice ($P < 0.001$, Figure 5E, left panel). The number of Zic$^-$ChAT$^+$ cells in the medial septum and Zic$^+$ChAT$^+$ cells in the diagonal band and medial septum region also tended to be reduced in *Zic2*$^{kd/+}$ mice compared to the wild type (Zic$^-$ChAT$^+$ cells in the medial septum, $P = 0.062$; Zic$^+$ChAT$^+$ cells in the diagonal band and medial septum region, $P = 0.12$ and $P = 0.056$ respectively). These results were consistent with those obtained in adult mice, suggesting that the reduction in the number of ChAT-positive neurons in the basal forebrain primarily stemmed from the reduction in *Zic2* gene expression during embryonic or prenatal development. In addition, we found that the number of Zic$^+$ChAT$^-$ cells was significantly increased in the diagonal band region and medial septum in *Zic2*$^{kd/+}$ mice compared to wild-type mice (diagonal band, $P = 0.039$; medial septum, $P = 0.047$ respectively; Figure 5E, right panel).

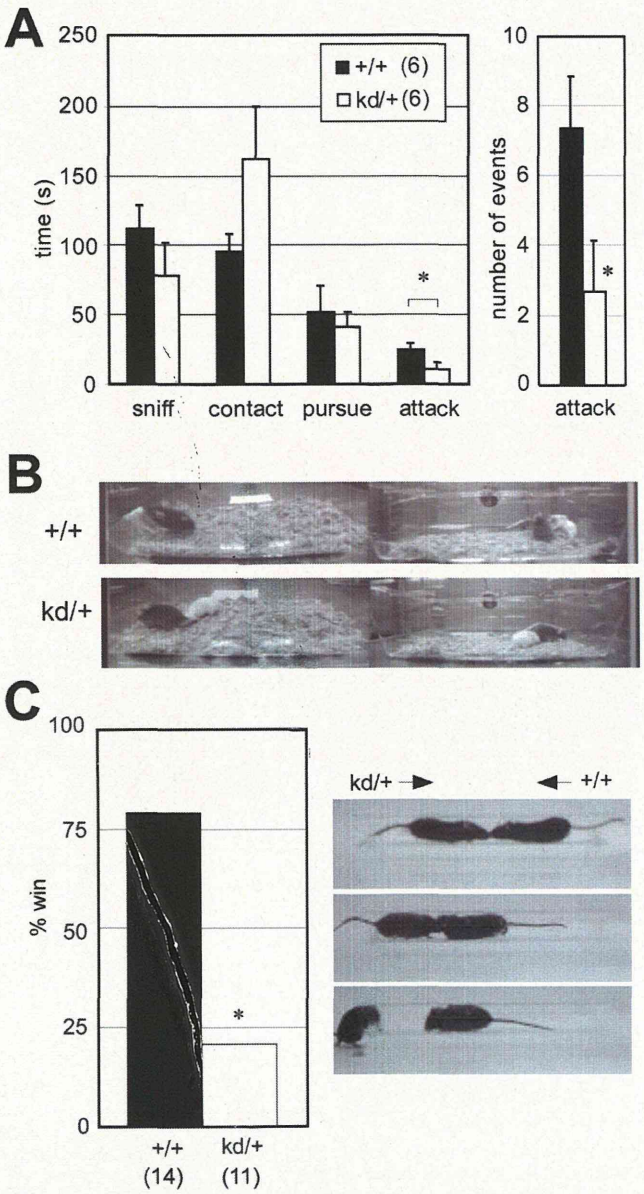

Figure 3 | Social behavior abnormalities in *Zic2*$^{kd/+}$ mice. (A) Resident-intruder test. (left) Total time spent in the indicated behaviors. (right) The number of attacking events. *$P < 0.05$ in t-test. Data is presented as means ± SEM. (B) Captured video image of the resident-intruder test. In this case, the *Zic2*$^{+/+}$ mouse (+/+, top, black) was attacking the white intruder mouse, whereas the *Zic2*$^{kd/+}$ mouse (kd/+, bottom black) was moving away from the intruder mouse. The left and right images indicate the simultaneous recording from opposite directions. (C) Social dominance tube test. (left) Won rate in the total of 66 matches. The means ± SEM latencies to win were as follows: *Zic2*$^{+/+}$, 36.5 ± 5.2; *Zic2*$^{kd/+}$, 38.3 ± 6.4 s. (right) Captured video images from a representative match. From top to bottom, the beginning to the end of the match is sequentially indicated. In this case, the *Zic2*$^{kd/+}$ mouse was pushed out from the plexiglass tube (30 cm) and the *Zic2*$^{+/+}$ mouse became the winner. *$P < 0.05$ in chi-square test. The number of mice in each group is given in parentheses.

Screening of *ZIC2* mutations in patients with schizophrenia. Some of the above behavioral and histological abnormalities in *Zic2*$^{kd/+}$mice are reminiscent of schizophrenia symptoms in humans. We therefore set out to examine whether *ZIC2* mutations contribute to the onset of schizophrenia, in at least a subset of patients. As a first step to address this possibility, we searched *ZIC2* for nonsynonymous mutations in patients with schizophrenia. Many nonsynonymous mutations are reported in patients with HPE[6,23]; however, there are no reports of an association of *ZIC2* mutations with psychiatric illnesses.

Sequence analysis of the entire *ZIC2* protein coding regions and adjacent introns in 278 patients revealed four nonsynonymous mutations in the coding regions (Table 2). We then examined the allele frequencies of these mutations in 967 patients with schizophrenia and in 1060 control subjects (Table 2). Ins239H was the most commonly detected mutation, but its frequency (~9%) was similar in patient and control groups. This finding is consistent with the results of previous studies[7,24–27]. The three remaining mutations, A95T, R409P, and S444R, were novel. A95T and R409P were singleton mutations not found in normal subjects. The frequency of S444R was not significantly different between the patient group (0.39%) and normal subjects (0.18%; $P = 0.80$ by Fisher's exact test). Patients with this mutation showed no obvious psychotic symptoms; however, we could not perform detailed physical examinations on these patients, nor examine the genotypes of their relatives because we could not obtain their consent on these issues.

The *Zic2*-R409P shows impaired transcriptional activation. Zic orthologues are widely distributed among the eumetazoans and show evolutionary conserved domains in their protein-coding regions[28]. Multi-species alignment of the three *Zic2* mutations revealed that R409P was located within the highly conserved regions of the published Zic sequences, including those of the protostomians and cnidarians (Figure 6A and data not shown). We also showed that R409 position has conserved in a zinc-finger-type transcription factor, GLI1, in which the side chain of the encoded amino acid residue is responsible for side-chain-base interactions (Figure S2)[29]. Both A95T and S444R were conserved in most of the vertebrate *Zic2* sequences examined, but these sequences did not align with those in invertebrates (Figure 6A and data not shown). We used the computer algorithm PolyPhen Polyphen[30] to predict the effect of the mutations on protein structure and function. PolyPhen analysis predicted that the amino acid change in R409P most likely caused abnormal protein structure and function, whereas it was only a possibility for S444R and even less likely for A95T (Table 2).

We characterized the function of these mutations by generating the equivalent mutations in mouse Zic2 proteins, and assessing their activities in vitro. The size of the mutant Zic2 proteins was mostly comparable to that of the wild type protein, as shown by sodium dodecyl sulfate-polyacrylamide gel electrophoresis (SDS-PAGE) analysis (Figure 6B). However, the band corresponding to Zic2-S444R also contained a fast migrating component in preparations from both transfected mammalian cells and from in vitro translation (Figure 6B and data not shown). The nuclear localization capacity of the mutant proteins was significantly reduced for R409P ($P < 0.001$ in chi-square test), but not for A95T or S444R (Figure S2). Zic2 can be a transcriptional activator[31,32]. We assessed the transactivating activity of the mutant proteins by co-transfecting mammalian cells with expression vectors that express the proteins. The Zic2-R409P protein, but not the Zic2-A95T or Zic2-S444R proteins had significantly reduced transactivating capacity compared to the wild-type protein ($P < 0.001$, Figure 6C); the normalized activation capacity of Zic2-R409P was approximately 20% that of the wild-type protein. When we examined the effect of the R409P mutation on the capacity to bind a high-affinity Zic-binding sequence, Zic2-R409P showed lower binding affinity to the target sequences than wild-type Zic2 (Figure 6D and 6E). Zic2 is known to complex with the DNA-PK catalytic subunit and RHA[33]. As shown in immunoprecipitation experiments (Figure 6F), the binding affinity of Zic2-R409P to DNA-PK, but not to RHA, was reduced compared to wild-type

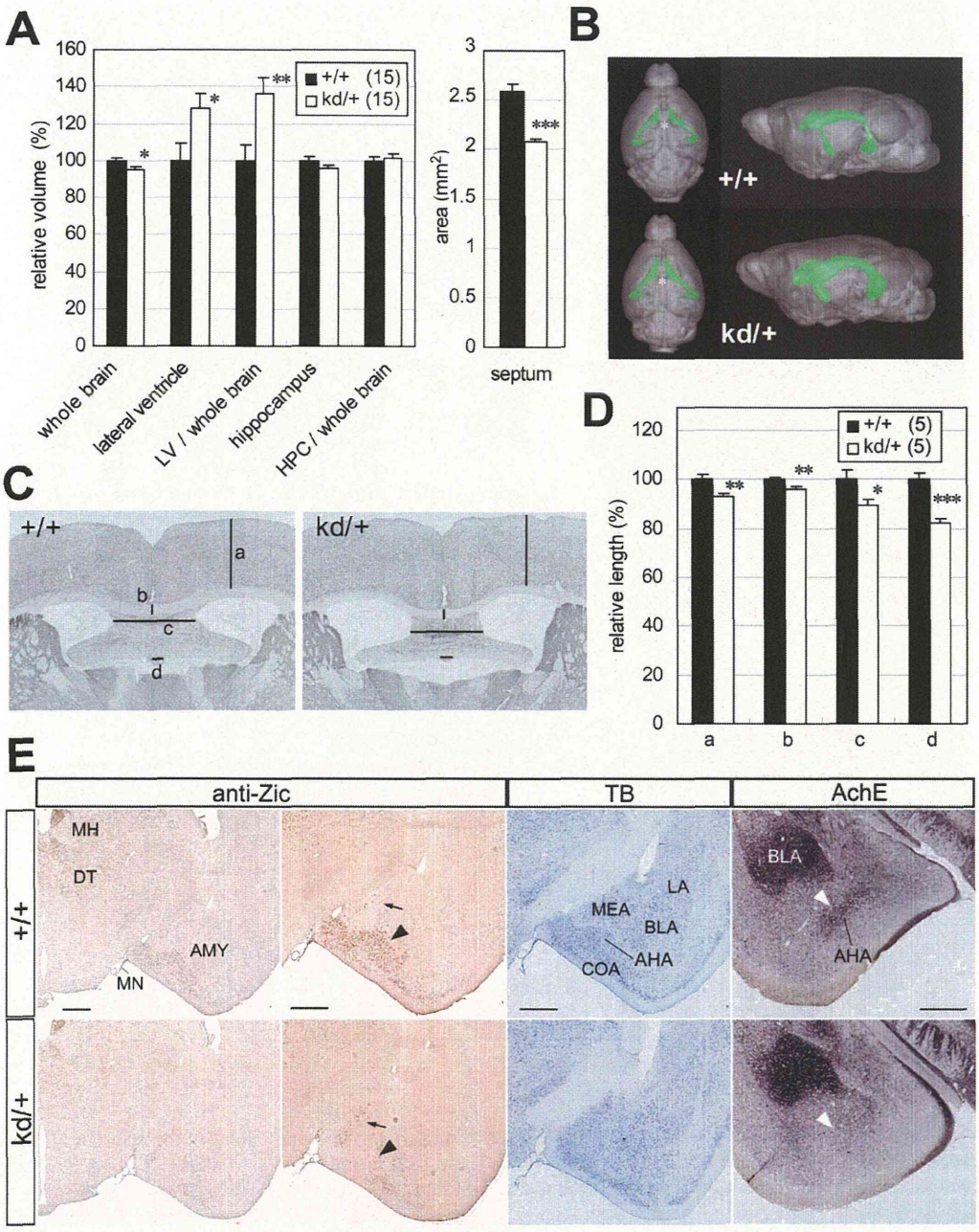

Figure 4 | Morphological features of the brains from *Zic2*$^{kd/+}$ mice. (A) Volumetric analysis of the entire brain, lateral ventricle (LV), and hippocampus (HPC). The values for tissue volumes in *Zic2*$^{kd/+}$ mice are indicated as percentages of the corresponding wild-type values. The values for ratio of volumes in LV/whole brain and HPC/whole brain are also indicated as percentages of the corresponding wild-type values. A total of 15 pairs of *Zic2*$^{+/+}$ and *Zic2*$^{kd/+}$ mice were subjected to in vivo MRI imaging. $*P < 0.05$, $**P < 0.01$, $***P < 0.001$ in t-test. Data is presented as means ± SEM. (B) 3D reconstruction of the outer surface of the brains of *Zic2*$^{+/+}$ (+/+) and *Zic2*$^{kd/+}$ (kd/+) mice (gray) with lateral ventricle (green). Dorsal (left) and anterior-lateral (right) views are indicated. Note the enlarged lateral ventricles and the narrowed interspace between the left and right lateral ventricles containing septum (asterisk). (C) Morphometric analysis. Sections were subjected to acetylcholine esterase staining. (a)–(d) Lines denote the distances measured in each section (a, cerebral cortex thickness; b, corpus callosum thickness; c, medial structure rostral to the hippocampus [fimbria including septofimbrial nucleus or septal triangular nucleus]; d, subfornical organ width). The measurements were done on 15 pairs of the most comparable from the serial sections of adult male *Zic2*$^{+/+}$ and *Zic2*$^{kd/+}$ mice brains. (D) Morphometric analysis. The lengths are presented as a percentage relative to the corresponding wild-type values. $*P < 0.05$, $**P < 0.01$, $***P < 0.001$ in t-test. Data is presented as means ± SEM. (E) Morphological abnormalities in the amygdala. The coronal sections from *Zic2*$^{+/+}$ (+/+) and *Zic2*$^{kd/+}$ (kd/+) mice were subjected to immunostaining with the anti-Zic antibody, toluidine blue (TB), and acetylcholine esterase staining (AchE). The black arrowhead and arrow indicate the Zic-positive cells in the amygdalohippocampal area (AHA) and medial nucleus, respectively. The white arrowheads indicate the enhanced AchE signals in the AHA. AMY, amygdalar complex; BLA, basolateral nucleus of amygdala; COA, cortical nucleus of amygdala; DT, dorsal thalamic nuclei; LA, lateral nucleus of amygdala; MEA, medial nucleus of amygdala; MH, medial habenular nucleus; MN, meningeal membrane. Scale bars, 0.5 mm.

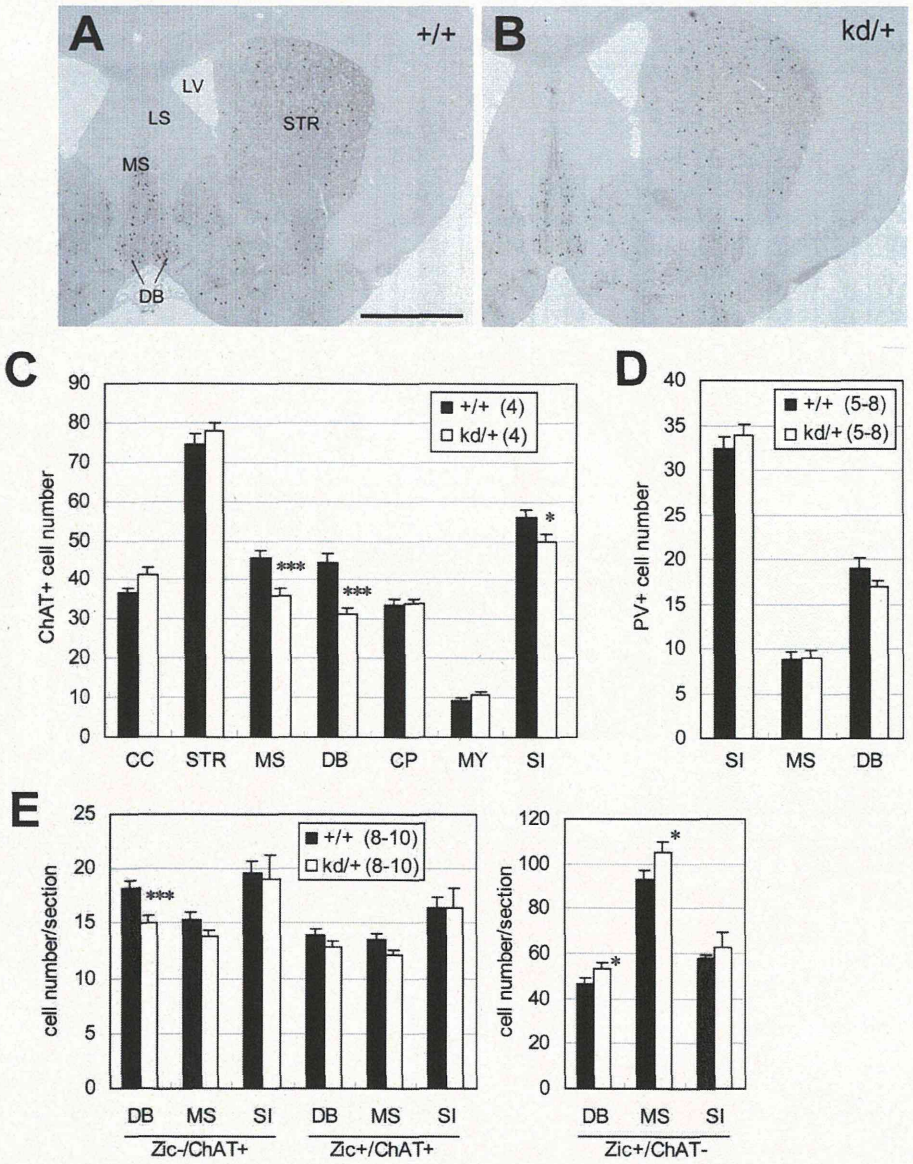

Figure 5 | Decreased number of cholinergic neurons in the brains of *Zic2*$^{kd/+}$ mice. (A,B) Immunostaining of the brains of *Zic2*$^{+/+}$ (+/+) (A) and *Zic2*$^{kd/+}$ (kd/+) (B) mice with anti-ChAT antibody. Coronal sections through the septum and diagonal bands derived from adult male mice were subjected to immunoperoxidase staining. Scale bar, 1 mm. (C) Number of the ChAT$^+$ neurons in the sections. Mean numbers of ChAT$^+$ neurons in 20 sections from the *Zic2*$^{+/+}$ and *Zic2*$^{kd/+}$ mice brains are indicated. (D) PV-positive cell numbers. The measurements were taken in comparable regions to those subjected to ChAT-immunostaining. (E) The numbers of ChAT- and Zic-immunoreactive neurons in early postnatal (P5-7) *Zic2*$^{+/+}$ and *Zic2*$^{kd/+}$ brains. Double labeling was performed with the anti-ChAT antibody and anti-pan Zic antibody. CC, cerebral cortex; CP, caudoputamen; DB, diagonal band; LV, lateral ventricle; LS, lateral septum; MS, medial septum; MY, Mynert nucleus; SI, substantia innominata; STR, striatum. (C–E) Data is presented as means ± SEM. The number of mice in each group is given in parentheses. *$P < 0.05$, ***$P < 0.001$ in t-test.

Zic2. Taken together, these results suggested that the R409P mutation dampens the transcriptional activation capacity of Zic2 by altering the properties of the Zic2-containing molecular complex.

Discussion

Our behavioral analysis in mice uncovered some novel roles of Zic2 related to higher brain function. A summary of the results from this behavioral analysis and that of previous studies is provided in Table 1.

The locomotor activity differences between wild-type and *Zic2*$^{kd/+}$ mice were context-dependent. In home cages, the mutant mice showed reduced locomotor activity in the early dark phase compared to wild-type mice, but in the open field test the mutant mice showed higher locomotor activity than wild-type mice. The tendency for *Zic2*$^{kd/+}$ mice to display higher activity in a novel environment, compared to wild-type mice was also observed in the the Y-maze test and the light-dark box test (Figure S1C). Therefore, *Zic2*$^{kd/+}$ mice appear to be generally hyperactive upon exposure to a novel environment. This hyperactivity is possibly consistent with symptoms of schizophrenia in humans; hyperactivity in response to a novel environment has been suggested as a useful animal correlate of schizophrenia symptoms[34] and has been noted in some genetically engineered mouse models of schizophrenia[35–37].

We demonstrated cognitive dysfunction in *Zic2*$^{kd/+}$ mice by the water maze test, the fear-conditioning test, and the Y-maze test. In addition, abnormal PPI, which is deemed to reflect impaired